

Cambridge University Press

978-1-107-41216-3 — Dislocations and Deformation Mechanisms in Thin Films and Small Structures

Edited by Oliver Kraft, Klaus W. Schwarz, Shefford P. Baker, L. Ben Freund, Robert Hull

Excerpt

[More Information](#)

---

**Dislocation and Deformation  
Mechanisms in Thin Metal Films  
and Multilayers I**

Mat. Res. Soc. Symp. Proc. Vol. 673 © 2001 Materials Research Society

### Constrained Diffusional Creep in Thin Copper Films

D. Weiss, H. Gao, and E. Arzt

Max-Planck-Institut für Metallforschung and Institut für Metallkunde der Universität,  
Seestr. 92, D-70174 Stuttgart, Germany

#### ABSTRACT

The mechanical properties of thin metal films have been investigated for many years. However, the underlying mechanisms are still not fully understood. In this paper we give an overview of our work on thermomechanical properties and microstructure evolution in pure Cu and dilute Cu-Al alloy films. Very clean films were produced by sputtering and annealing under ultra-high vacuum (UHV) conditions. We described stress-temperature curves of pure Cu films with a constrained diffusional creep model from the literature. In Cu-1at.%Al alloy films, Al surface segregation and oxidation led to a "self-passivating" effect. These films showed an increased high-temperature strength because of the suppression of constrained diffusional creep; however, under certain annealing conditions, these films deteriorated due to void growth at grain boundaries.

#### INTRODUCTION

For many years, materials research has focused on the understanding of deformation mechanisms in thin metal films on stiff substrates (see [1] and [2] for an overview). Copper and aluminum films on silicon substrates have been of special interest, as these materials are used today for microchip metallization. The large difference in thermal expansion coefficients of the film and substrate materials can lead to mechanical film stresses up to several 100 MPa, which are considered a serious reliability issue in microelectronic industry. Basic research has been interested in two specific phenomena: First, thin-film yield stresses at low temperatures are often proportional to the inverse of the film thickness. This effect has been explained in terms of a dimensional constraint on dislocation motion [1]. Second, the particular shape of a stress-temperature curve under thermal cycling depends not only on the film material, but can also change substantially if the film surface is protected by a thin protection layer (so called passivation) [3].

In this paper we report on the dramatic effect of vacuum conditions during film synthesis on the thermomechanical behavior and the microstructure of pure Cu films. Films produced under UHV conditions supported much higher stresses at high temperatures than conventional films produced under high-vacuum (HV) conditions. Stress-temperature curves of the UHV-produced Cu films could be well described with constrained diffusional creep. We furthermore report on alloying effects in Cu-1at.%Al films. Al surface segregation and oxidation led to a "self-passivating" effect. Stress-temperature curves were more "square" than the curves of pure Cu films and apparent signs of constrained diffusional creep were absent in these films. We also show that, under certain annealing conditions, large voids can grow at grain boundaries and grain-boundary triple junctions of the alloy films. A growth mechanism based on grain-boundary diffusional creep is discussed.

## EXPERIMENT

Pure Cu films with thicknesses of 0.5 and 1  $\mu\text{m}$  were produced by DC magnetron sputtering under UHV conditions (base pressure  $1 \times 10^{-8}$  Pa, 99.997% purity of Cu target). 2" Si wafers in (100) orientation, coated on both sides with 50 nm-thick amorphous  $\text{SiO}_x$  and  $\text{SiN}_x$  diffusion barriers, were used as substrates. Film synthesis, which is described in greater detail in [4], consisted of three steps: substrate cleaning by Ar ion bombardment, film deposition, and annealing (10 min at 600  $^\circ\text{C}$ ). UHV conditions were maintained between all three steps. The sputtering gas (Ar) was further purified by a chemisorptive gettering system. Cu-1at.%Al films were produced in the same chamber by co-sputtering from a pure Al target (99.999% purity). After annealing, some films were oxidized at different temperatures and controlled oxygen pressures.

The microstructure of the films was analyzed with focused ion beam microscopy (FIB, FEI 200 workstation), transmission electron microscopy (TEM, JEOL 200CX), standard X-ray methods (Siemens D5000), Auger depth profiling, and X-ray photoelectron spectroscopy (XPS).

The mechanical film properties were measured during thermal cycling using the wafer curvature technique [5]. A wafer was placed on a tripod in a furnace continuously purged with nitrogen. Temperature was linearly increased from room temperature to either 500 or 600  $^\circ\text{C}$  at a rate of 6 K/min. Wafer curvature, which is proportional to film stress, was measured with a laser-scanning system.

## RESULTS AND DISCUSSION

### Mechanical behavior and microstructure of UHV-sputtered Cu and Cu-1at.%Al films

In Figure 1a, three stress-temperature curves of different 1  $\mu\text{m}$  thick Cu films on Si substrates are compared. Both vacuum conditions during film synthesis and Al alloying have a large influence on the mechanical film properties. Thermal stress evolution in the pure Cu film, sputtered and annealed under UHV conditions, clearly differs from that in a Cu film fabricated at conventional HV conditions (Ref. [6]): the UHV Cu film supports significantly higher stresses than the HV film. Even higher stresses are found in the film alloyed with 1at.%Al. All these phenomena are due to different types of plastic deformation, which will be discussed below. Where thermal mismatch strain is accommodated mainly elastically, all curves are of similar shape. This occurs at the beginning of the heating cycle.

Vacuum conditions during film synthesis also had a large influence on the post-annealing microstructure. In contrast to HV Cu films known from the literature, which have a small grain size, mixed grain texture, and many twins [6], the UHV Cu films from this work had a larger grain size (median grain size 2.4  $\mu\text{m}$  for a 1  $\mu\text{m}$  thick film), very few twins (see Figure 1b), and a very strong and sharp {111} texture (see inset in Figure 1b).

The curve of the Cu-1at.%Al alloy film in Figure 1a looks similar to that of pure Al films known from the literature [7]. We found that surface segregation and oxidation of Al atoms during film oxidation led to a "self-passivating" effect, which is also described in the literature [8]. As we show in the following, the difference in high-temperature stresses between the Cu-Al alloy films and the pure Cu films can be quantitatively described by constrained diffusional creep, which is believed to be suppressed by the aluminum-oxide passivation in the alloy films.

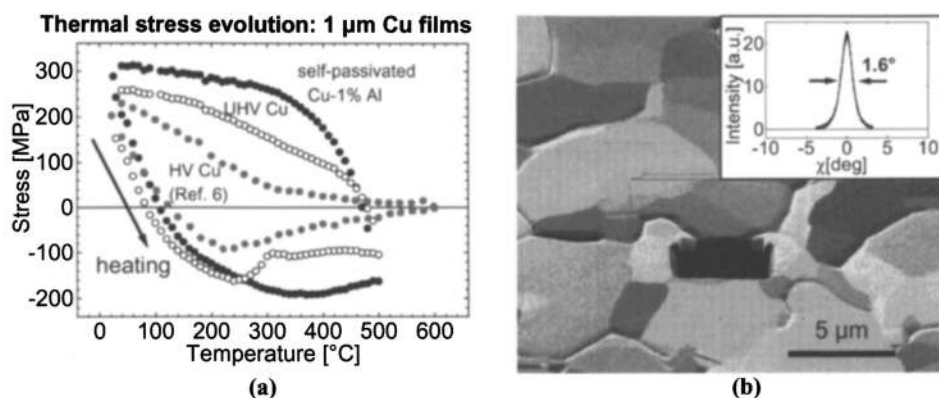


**Figure 1** (a) Stress-temperature curves for 1 μm thick pure Cu and Cu-1at.%Al films (UHV, this work) and for a pure Cu film (HV, data taken from Keller et al., Ref. [6]). (b) FIB micrograph of 1 μm thick UHV-sputtered and annealed Cu film (with sputter-etched trench, sample tilt 45°). Inset: X-ray rocking curve of the {111} reflection of a similar film.

### The constrained diffusional creep model

Grain-boundary diffusional creep in thin films has been the subject of many publications [9–12]. Recently, Gao and coworkers have presented a closed-form solution of constrained diffusional creep in films with columnar grains [13]. For the first time this problem has been solved for the constraint of perfect film adhesion, i.e. no sliding and no diffusion at the film/substrate interface was allowed. A schematic of this mechanism is shown in Figure 2a (top). Surface atoms, transported into the grain boundaries by directed diffusion under tensile stress, give rise to the formation of so called diffusion wedges at the grain boundaries: as a result of perfect film adhesion, the stress is relaxed more efficiently at the grain boundaries and at the film surface than in the grain interior and at the film/substrate interface.

Fast surface diffusion is required for constrained grain-boundary diffusional creep. The inhibition of surface diffusion would hence lead to an inhibition of this creep mechanism (Figure 2a, bottom). It is therefore plausible that constrained diffusional creep would be suppressed in the self-passivated Cu-Al alloy films. This also explains the similarity between the Cu-1at.%Al and Al films: Al is de facto passivated by the native oxide [3,14].

Figure 2b shows the theoretical stress evolution in a 0.5 μm thick Cu film, if constrained diffusional creep was the only plastic deformation mechanism. Similar results have been previously published by Dalbec et al. [15]. The average grain-boundary stress, shown as a dotted line, fully relaxes to zero at high temperatures. A similar curve would be obtained for the stress in a free-standing film, i.e. a film *without* substrate constraint. In contrast, the average stress in a film perfectly attached to the substrate (solid line in Figure 2b) does not relax to zero – even for fully relaxed grain boundaries.

A model for the stress evolution in Cu films should consider dislocation glide as well. We have recently suggested a modeling procedure schematically shown in Figure 3a [16]. Here, the reference stress  $\sigma_0$ , which is the stress in a film *without* diffusion wedges, is described by a

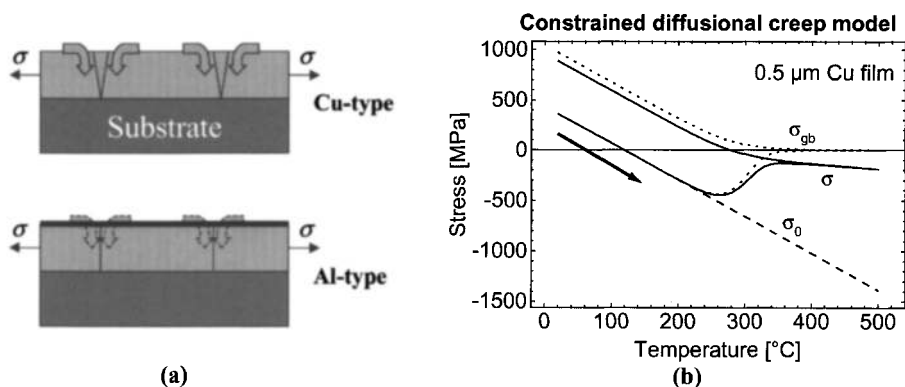


**Figure 2** (a) Schematic for constrained diffusional creep under tensile stress (top). The grey arrows indicate atomic diffusion; the direction of diffusion would be reversed for compressive stress. A surface layer suppressing surface diffusion leads to the inhibition of constrained diffusional creep (bottom). (b) Modeled stress-temperature curve for a 0.5  $\mu\text{m}$  thick Cu film with constrained diffusional creep as the only relaxation mechanism.  $\sigma_{gb}$  is the average grain boundary stress,  $\sigma_0$  is a reference stress for a similar film without diffusion wedges, and  $\sigma$  is the average stress. The equations and model parameters are found in Ref. [16].

polynomial fit of the *experimental* stress  $\sigma_p$  of a self-passivated film of similar thickness. Grain-boundary stress and average stress are obtained numerically by solving the equations for constrained diffusional creep. In other words, we calculate the amount of stress which would be relaxed by constrained diffusional creep, if the passivation of the same film was removed. As a simplification, we neglected any influence of local stress relaxation by creep on dislocation glide. Figure 3b shows that the resulting average stress compares considerably well with the experimental data of an unpassivated film. As the only fitting parameter, grain size was chosen almost three times larger than the median grain size obtained by quantitative microstructure analysis. This larger effective grain size might be explained by unrelaxed low-energy boundaries.

### Creep voiding in self-passivated Cu-1at.%Al films

In Cu-1at.%Al alloy films oxidized at or above 500  $^{\circ}\text{C}$ , large voids were found at many grain boundaries and grain-boundary triple junctions. Figure 4a shows a TEM image of a void at a triple junction in a Cu-1at.%Al film, which was annealed and subsequently oxidized at 600  $^{\circ}\text{C}$  in the sputtering chamber. A plausible growth mechanism is the diffusion of atoms from the surface of a void, nucleated at the intersection of a grain boundary with the surface oxide, into the grain boundary [17]. Driving force for void growth is the tensile film stress developing upon cooling. The inset in Figure 4a illustrates this mechanism, which is related to creep voiding in bulk alloys [18].

Figure 4b shows crack-like voids at grain boundaries and triple junctions in a similar film that was oxidized under less controlled conditions during thermal cycling to 600  $^{\circ}\text{C}$  in the wafer-curvature apparatus. Here, continuous oxidation of void surfaces during cooling caused the

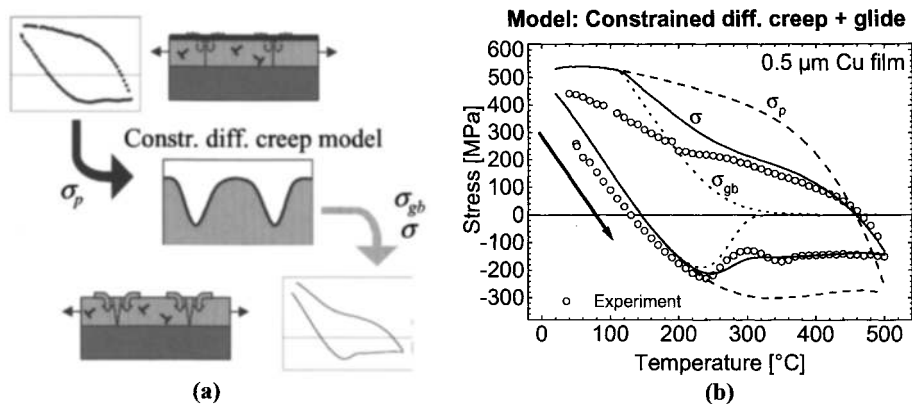


**Figure 3 (a)** Schematic for modeling constrained diffusional creep together with dislocation glide.  $\sigma_p$  is the experimental stress of a self-passivated film. **(b)** Model result in comparison with experimental data of a 0.5  $\mu\text{m}$  thick unpassivated Cu film. A detailed description of the calculation is found in Ref. [16].

crack-like void shape. This particular void shape is also predicted for creep voids in bulk alloys, if diffusion on the void surface is rate limiting [18].

Grain-boundary voids were found neither in *unalloyed* Cu films, oxidized at 600 °C, nor in Cu-Al alloy films, annealed but *not oxidized*. Both systems exhibit high diffusivity at the film surface, which is why constrained diffusional creep, without the nucleation of voids, is energetically more favorable. Stress voiding can be a serious technological problem in thin conductor lines, where high tensile stresses may develop. Our results have unambiguously shown that this detrimental effect can be avoided in passivation-free films or by careful choice of the annealing parameters.

## CONCLUSIONS

We have shown that synthesis of pure Cu films under very clean UHV conditions had large effects on both the thermomechanical behavior and the microstructure of these films. Stress-temperature curves displayed high residual stresses even at high temperatures. These curves were for the first time successfully described by a constrained diffusional creep model. Cu films alloyed with 1at.%Al supported even higher high-temperature stresses. Surface segregation and oxidation of Al atoms led to a self-passivating effect, which is believed to inhibit constrained diffusional creep. Cu-Al alloy films, annealed and oxidized at temperatures at or above 500 °C, were degraded due to voiding at grain boundaries and grain-boundary triple junctions. This detrimental effect can be avoided in passivation-free films or by careful choice of the annealing parameters.

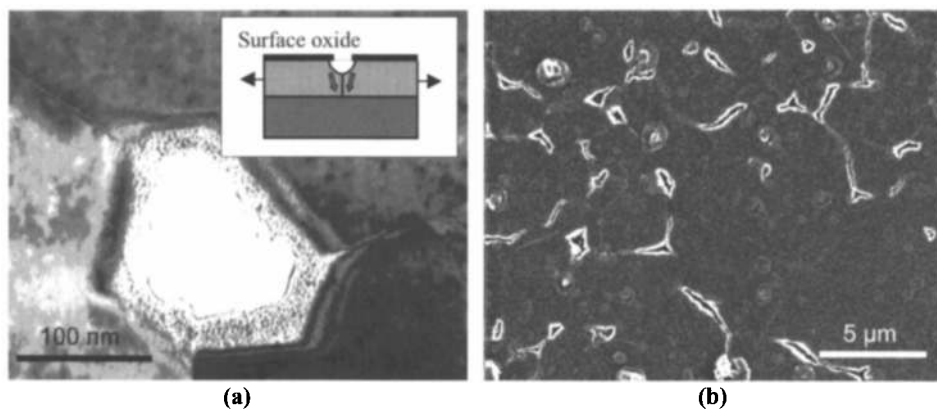


**Figure 4** (a) TEM plan-view micrograph showing a void at a grain-boundary triple junction in a Cu-1at.%Al film, oxidized in the UHV sputtering chamber. Inset: Cross section of grain-boundary void (schematic). (b) FIB micrograph of crack-like voids in a 1  $\mu\text{m}$  thick Cu-1at.%Al film, oxidized during thermal cycling to 600  $^{\circ}\text{C}$  in the furnace of the wafer curvature apparatus.

## ACKNOWLEDGEMENTS

The authors acknowledge fruitful discussions with S. Baker, K.-N. Tu, O.S. Leung, W.D. Nix, M.J. Koblinsky, and C.V. Thompson. This work was supported by the Deutsche Forschungsgemeinschaft under contract number AR 201/5.

## REFERENCES

1. W. D. Nix, *Metall. Trans. A* **20A**, 2217-45 (1989).
2. E. Arzt, *Acta Mater.* **46**, 5611-26 (1998).
3. M. D. Thouless, K. P. Rodbell, and C. J. Cabral, *J. Vac. Sci. Tech. A* **14**, 2454-61 (1996).
4. D. Weiss, PhD Thesis, Universität Stuttgart (2000).
5. P. A. Flinn, D. S. Gardner, and W. D. Nix, *IEEE Trans. Electr. Dev.* **ED-34**, 689-99 (1987).
6. R.-M. Keller, S. P. Baker, and E. Arzt, *J. Mater. Res.* **13**, 1307-17 (1998).
7. Y.-C. Joo, P. Müllner, S. P. Baker, and E. Arzt, *MRS Symp. Proc. Vol. 473*, (Philadelphia, PA, 1997), p. 409-14.
8. J. Li, J. W. Mayer, and E. G. Colgan, *J. Appl. Phys.* **70**, 2820-7 (1991).
9. G. B. Gibbs, *Phil. Mag.* **13**, 589-93 (1966).
10. M. S. Jackson and C.-Y. Li, *Acta Met.* **30**, 1993-2000 (1982).
11. M. D. Thouless, *Acta Met.* **41**, 1057-64 (1993).
12. M. J. Koblinsky and C. V. Thompson, *Appl. Phys. Lett.* **73**, 2429-31 (1998).
13. H. Gao, L. Zhang, W. D. Nix, C. V. Thompson, and E. Arzt, *Acta mater.* **47**, 2865-78 (1999).
14. R. P. Vinci, E. M. Zielinski, and J. C. Bravman, *Thin Solid Films* **262**, 142-53 (1995).
15. T. R. Dalbec, O. S. Leung, and W. D. Nix, in *Deformation, Processing, and Properties of Structural Materials*, edited by E. M. Taleff, C. K. Syn, and D. R. Lesuer (The Minerals, Metals & Materials Society, 2000), p. 95-108.
16. D. Weiss, H. Gao, and E. Arzt, *Acta mater.*, in press (2001).
17. D. Weiss, O. Kraft, and E. Arzt, *Appl. Phys. Lett.*, submitted (2001).
18. A. C. F. Cocks and M. F. Ashby, *Progr. Mat. Sci.* **27**, 189-244 (1982).



## An Experimental and Computational Study of the Elastic-Plastic Transition in Thin Films

Erica T. Lilleodden<sup>1</sup>, Jonathan A. Zimmerman<sup>2</sup>, Stephen M. Foiles<sup>3</sup> and William D. Nix<sup>1</sup>

<sup>1</sup>Department of Materials Science & Engineering, Stanford University, Stanford, CA 94305-2205, <sup>2</sup>Sandia National Laboratories, Livermore, CA 94551, <sup>3</sup>Sandia National Laboratories, Albuquerque, NM 87185

### ABSTRACT

Nanoindentation studies of thin metal films have provided insight into the mechanisms of plasticity in small volumes, showing a strong dependence on the film thickness and grain size. It has been previously shown that an increased dislocation density can be manifested as an increase in the hardness or flow resistance of a material, as described by the Taylor relation [1]. However, when the indentation is confined to very small displacements, the observation can be quite the opposite; an elevated dislocation density can provide an easy mechanism for plasticity at relatively small loads, as contrasted with observations of near-theoretical shear stresses required to initiate dislocation activity in low-dislocation density materials. Experimental observations of the evolution of hardness with displacement show initially soft behavior in small-grained films and initially hard behavior in large-grained films. Furthermore, the small-grained films show immediate hardening, while the large grained films show the ‘softening’ indentation size effect (ISE) associated with strain gradient plasticity. Rationale for such behavior has been based on the availability of dislocation sources at the grain boundary for initiating plasticity. Embedded atom method (EAM) simulations of the initial stages of indentation substantiate this theory; the indentation response varies as expected when the proximity of the indenter to a  $\Sigma 79$  grain boundary is varied.

### INTRODUCTION

Length-scale is fundamentally important to materials science, as evidenced by its relation to microstructure-property relations. For example, the flow stress of a material is known to scale with the square root of the dislocation density, inversely with the square root of the grain size, and, in the case of thin films, inversely with film thickness. However, a single-valued flow stress, considered to be a material property, is typically used in continuum mechanics. This removes any explicit length-scale dependence from the constitutive relations, taking into account only the average microstructure of the material. This is a reasonable approach in cases where the scale of deformation is large relative to the scale of microstructural inhomogeneities. However, as the characteristic length-scale of the deformation field tends toward the characteristic material length-scale, the governing relations between stress and strain may deviate from classical laws. Indeed, anomalous yielding behavior has been commonly observed in nanoindentation studies. Discrete load-displacement response in the early stages of indentation (e.g. several nanometers to tens of nanometers) has been widely observed [e.g. 2, 3, 4], and can be associated with the nucleation of dislocations. At a larger length-scale (>100nm) the observation of decreasing hardness with increasing displacement can be explained by strain gradient plasticity [e.g. 1]. However, both of these anomalies are most easily discussed without explicitly considering the microstructure of the indented materials. It is thus the objective of this work to explore the effect of microstructure on the initiation and evolution of plasticity.



## EXPERIMENTAL

The experimental work was accomplished with a 1 micron gold film evaporated onto a Si (001) substrate, and a 0.16 micron thick gold film sputtered onto an amorphous silica substrate. Both films showed strong (111) texture. The silica substrate was used for the thinner film in order to minimize substrate effects, since silica and gold have similar elastic properties. The absence of a native oxide layer makes gold an ideal system for studying the onset of plasticity, since the absence of an oxide removes the possibility of oxide fracture or other oxide/metal interface defect effects. The films were annealed in order to grow the grains and to remove any pre-existing dislocations from the grain interiors. A 3 to 4nm W layer was deposited on the bare substrates, to promote adhesion of the films. Atomic Force Microscopy (AFM) was used to characterize the grain size and surface roughness of the samples. The 1 micron thick film had a grain size roughly 2 to 3 times the film thickness, while the 0.16 micron thick film had a grain size on the order of the film thickness. Nanoindentation experiments were conducted with a Nanoindenter XP with a DCM head (MTS, Minneapolis, MN). This instrument provides a continuous measurement of the contact stiffness via a superimposed oscillation of the load during loading. The continuous stiffness measurement (CSM) technique [5] greatly improves the function of nanoindentation experiments, by offering continuous measurement of the elastic and plastic response of the material during loading, rather than relying a set of partial unloading curves and/or multiple indentations for valid characterization. This technique is critical to understanding the evolution of plasticity during a single indentation, which is important in understanding the dependence of plastic deformation on local microstructural environment.

## RESULTS AND DISCUSSION

Figure 1 compares the indentation behavior of the small grained 0.16 micron thick Au/silica sample and the large grained 1 micron Au/Si sample. Several distinct differences are clearly observed. The 1 micron thick film shows elastic discrete load-displacement behavior and larger sustained loads in the initial stages of deformation. In contrast, the small grained film shows continuous loading, with no discrete transition between elastic and plastic deformation. The hardness was measured in the conventional way, using a calibrated indenter-tip area function for the calculation of the contact area. The difference in hardness-displacement behavior between the two samples is particularly striking. The development of the mean pressure (defined as the indentation hardness, but not necessarily associated with plastic deformation) in the 1 micron thick film during elastic loading reaches a value of 2.2 GPa, whereas the polycrystalline film shows initially soft behavior and a hardness of 0.5 GPa. Following the first pop-in during indentation into the 1 micron thick film, the hardness is observed to decrease, as may be ascribed to continued dislocation nucleation or strain gradient plasticity effects. In contrast, the small grained film shows increased hardness with increasing displacement. The increased hardness can be attributed to conventional Hall-Petch behavior upon inspection of the number of grains contacted during loading, as shown in Figure 1(d). Dividing the contact area by the average grain size reveals multigrain contact in the case of the 0.16 micron thick film, while the 1 micron film is well described by single crystal behavior, within the first 100nm of displacement.

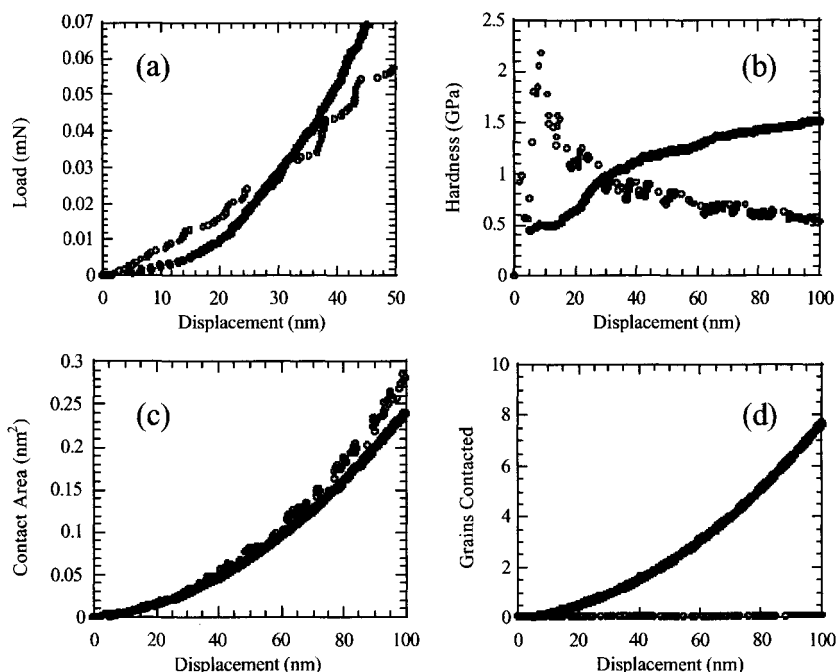


**Figure 1.** (a) Load and (b) hardness behavior of the 1 micron thick Au film on Si (open circles), and the 160nm small grained Au film on silica (filled circles), show significant differences. Assessment of the (c) contact area and subsequently (d) the number of grains contacted during indentation reveal a Hall-Petch type hardening mechanism in the small grained sample, while the large grained film shows the nucleation and strain gradient effects associated with single crystal behavior.

The differing behavior of the two films can be rationalized in terms of the availability of dislocation sources. Grain boundaries may act as effective dislocation sources, rather than requiring high energy-cost nucleation events to initiate plasticity. Thus, indentations into volumes that include or are near a grain boundary may allow easy initiation of plasticity. Consistent with this theory, the small grained film shows continuum elastoplastic behavior immediately, in contrast to the discrete elastic-plastic transitions observed in the large grained film. Additionally, the small grained film showed reproducible load-displacement behavior for random indentation positions across the sample. This is in sharp contrast to the load-displacement sensitivity to grain boundary proximity for the larger grained 1 micron thick film. Figure 2 shows the load-displacement behavior of two indentations: one indent positioned in the center of a grain, and another indent positioned close to the grain boundary. It is revealed that the indentation into the center of the grain leads to a higher critical load for pop-in and smaller overall displacements during the initial stages of plastic deformation, as compared with the indentation near the grain boundary.